Proc. of the Int. Workshop on Nuclear Data for the Transmutation of Nuclear Waste, GSI-Darmstadt, Germany, Sept. 1-5, 2003, ISBN3-00-012276-1.

Development of the Photonuclear Activation Data Library for CINDER'90

M.-L. GIACRI-MAUBORGNE, D. RIDIKAS*, J.-C. DAVID
CEA/Saclay, DSM/DAPNIA/SPhN, F-91191 Gif/Yvette, France
M. B. CHADWICK, W. B. WILSON
Los Alamos National Laboratory (T-16), Los Alamos, NM 87545, USA

In this article we present the development of a photonuclear activation data library for CINDER'90. The IAEA evaluations for 164 nuclei are included explicitly and reactions for another ~500 isotopes are added using the HMS-ALICE predictions. We also test the GNASH code for some evaluations in the case of actinides. Some preliminary calculations of photo-fission yields are done with the GSI fission-evaporation program. Finally, the transmutation analysis of nuclear waste in high photon fluxes is performed as a test case of the newly developed photonuclear data library.

INTRODUCTION

Recently a renewed interest in photonuclear processes has appeared. It is motivated by a number of different applications where progress in high intensity electron accelerators was awaited$^{1)}$. Major problems in modelling photonuclear reactions are the lack of photonuclear data on corresponding cross sections despite the huge efforts of the IAEA$^{2)}$, where data are available for 164 isotopes. In addition, no material evolution code including photonuclear reactions is available.

For this reason, in a close collaboration with the LANL, we have been working on the development of a new photonuclear activation data library to be included into the CINDER'90$^{3)}$ evolution code. HMS-ALICE$^{4)}$ and GNASH$^{5)}$ have been used to calculate photonuclear reactions for more than 500 isotopes. For photo-fission fragment distributions we test the fission-evaporation code from GSI$^{6)}$ known to give good results in the case of high energy spallation reactions. Finally, as a case study, we use the newly developed photonuclear data files to perform a feasibility study of the transmutation analysis in γ-fluxes for some long-lived fission fragments and minor actinides. These results are compared to the equivalent estimates in high neutron fluxes.

PHOTONUCLEAR ACTIVATION LIBRARY FOR CINDER'90

CINDER'90 initially was developed to perform the activation analysis in neutron fluxes. By adding a photonuclear activation data library calculations can be done both in neutron and photon fluxes making the code a multi-particle activation program. Next improvements in CINDER'90 will consist in building a proton activation data library.

The following photonuclear library construction strategy was chosen:

a) we use the IAEA evaluations explicitly for the major 164 isotopes;
b) the latest version of the ALICE code (HMS-ALICE) written by M. Blann is employed to complete the library for nearly 600 isotopes;
c) in some particular cases new evaluations with the GNASH code are performed (e.g., ^{235}U, ^{239}Pu, ^{237}Np);
d) the GSI fission-evaporation code is used to provide the photo-fission fragment distributions.

The energy range of incident photons is between 0 and 25 MeV, and an extension of the present activation library up to 150 MeV is planned in the future. Our primary task during the construction of the data library was to test the accuracy of the calculated cross sections through comparisons with the existing experimental data and IAEA evaluations. Below we present our major findings.

HMS-ALICE predictions

HMS-ALICE is a multiparticle reaction code. In practice, it was used to calculate cross sections for nuclei heavier than ^{9}Be in the energy range from a few keV to the pion mass threshold. The major advantage of this program is that the results can be obtained very quickly for a big number of nuclei.

---

* ridikas@cea.fr

Below we compare the HMS-ALICE predictions for light, intermediate and heavy nuclei with the IAEA evaluations.

Carbon and aluminum are the most frequently used materials among the light nuclides. Figs. 1-2 present our results for ^{12}C and ^{27}Al. In brief, for ^{12}C, (γ,1n) and (γ,1p) the cross sections are largely underestimated. Contrary, we found that other reaction channels as (γ, α) are overestimated in the same simulation. For ^{27}Al the situation is opposite: the neutron emission is overestimated, while proton production is in a rather good agreement with data. The obtained differences are difficult to explain at the moment. However, it is clear that HMS-ALICE needs some improvements to predict the photonuclear reactions for light nuclei.

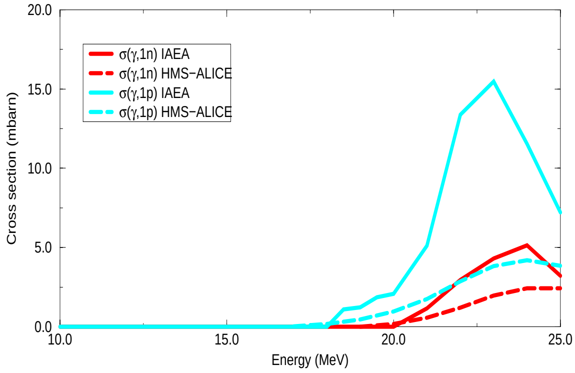

Fig. 1: Particle production for ^{12}C obtained with HMS-ALICE (dashed lines) and compared with the IAEA evaluations (solid lines).

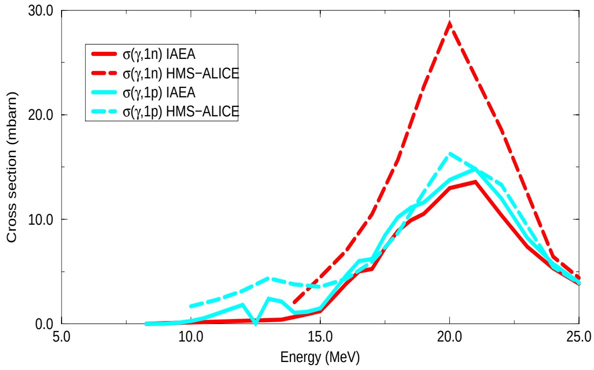

Fig. 2: Same as Fig. 1 but for ^{27}Al.

In the case of heavy nuclei we study ^{208}Pb because it is often used in nuclear technology for shielding purposes. In addition, it is a potential candidate for photoneutron production target. Finally, the existing data for this nucleus are of good quality. Our results are presented in Fig. 3. The ^{208}Pb cross section has a very regular shape and is very close to the model predictions in the entire energy range considered. Contrary, Fig. 4 (in the case of ^{181}Ta) shows some inconsistency between the IAEA evaluation and HMS-ALICE results for the (γ,1n). We believe that this discrepancy is directly related to the modelling of the total absorption cross section. Indeed, the IAEA evaluation gives an absorption cross section with two peaks whereas the HMS-ALICE model for absorption cross section is based on a single lorentzian. It is known that in the case of deformed nuclei, the total absorption cross section should be modelled by the sum of two lorentzians. As particle emission cross sections are based on total absorption cross section, they can not be reproduced properly for deformed nuclei.

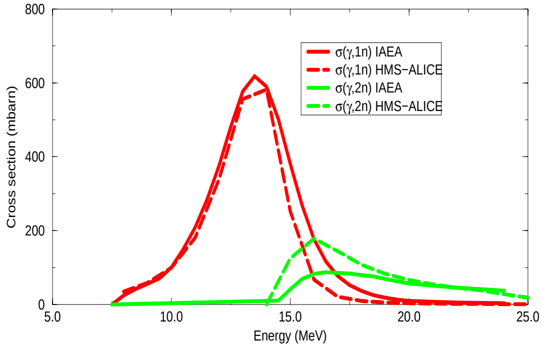

Fig. 3: Same as Fig. 1 but for ^{208}Pb.

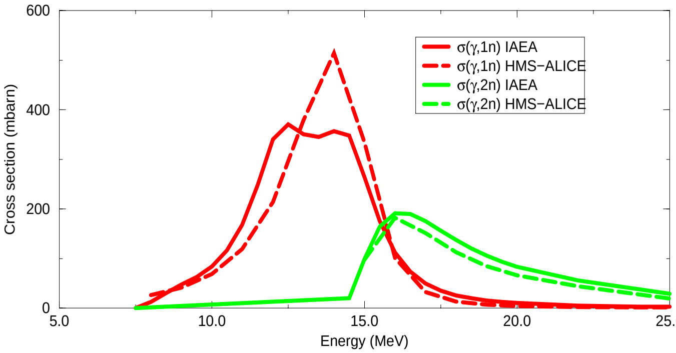

Fig. 4: Same as Fig. 1 but for ^{181}Ta.

This is in particular true for the actinides as shown in Fig. 5. Here we clearly confirm that the HMS-ALICE predictions are based on a single lorentzian, so they have only one peak, whereas all IAEA evaluations (based on experimental data) have two peaks.

Based on these findings we have tried to look for another model to calculate the total photo absorption cross section for actinides. For this purpose we employ the absorption cross section expressed as a sum of the giant dipole and giant quadruple resonance components, each of them determined from the empirical systematic (the same approach is used in the GSI fission-evaporation code). In addition, we tried to improve this description in terms of the deformation parameter, which influences the energy position of the resonance peak and the width of the lorentzian (see Fig. 6). Our results are encouraging and show a clear improvement of the σ_{abs} modelling. Therefore, we use this formulation for the remaining actinides where experimental data are not available.

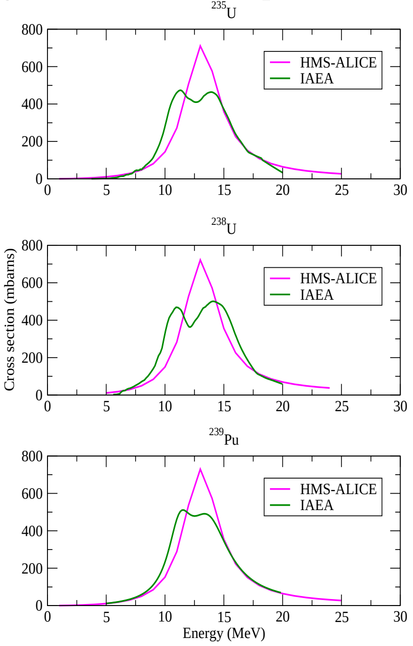

Fig. 5: Comparison of the HMS-ALICE's model for photoabsorption (in purple) with the IAEA evaluations (in green) in the case of actinides.

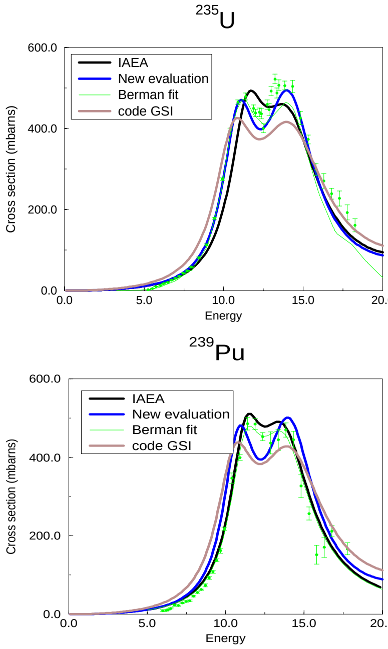

Fig. 6: Comparison of a modified GSI model with the IAEA evaluation, original GSI model and experimental data for ^{239}Pu and ^{235}U.

We conclude that HMS-ALICE is a powerful tool to calculate quickly desired photonuclear reaction cross sections. On the other hand, it should be used with a certain caution. In some cases the predicting power of this code is not sufficient and further development of physics models is needed.

Evaluations with GNASH

GNASH is another nuclear reaction code, which is based on the Hauser-Feshbach statistical approach including a pre-equilibrium stage. It requires as input ground state spin, parity, masses, nuclear structure data, particle transmission coefficients, etc. The absorption cross section is not necessary but is strongly recommended for photonuclear reactions to be confident in the output results. An advantage of GNASH is that its results can be prepared easily in the ENDF format and used directly in the transport codes.

During the computational procedure we employed similar approach as in the case of the calculations developed for neutron induced reactions with GNASH. For incident photons we suppressed the neutron absorption channel and added the total absorption cross section as input. Finally, experimental photonuclear cross sections are fitted by adjusting a number of physical parameters such as fission barrier and level density cards.

In Fig. 7 we present the GNASH evaluations for ^{235}U. The total photo-absorption cross section from IAEA was taken as input. For partial neutron production channels, including photo-fission, the experimental data up to 15 MeV are well reproduced. This result also serves to validate our computational procedure employed with GNASH.

Encouraged by the results for ^{235}U we also performed similar evaluations for ^{237}Np, for which no IAEA evaluations were made. Two independent measurements of total absorption cross section of ^{237}Np do exist, however the data are inconsistent$^{7)}$ as shown in Fig. 8. We decided to weight the two fits of experimental data to obtain an integral value in agreement with integral value of neighbour nuclei. The black curve in Fig. 8 is the total absorption cross section we used in the GNASH input.

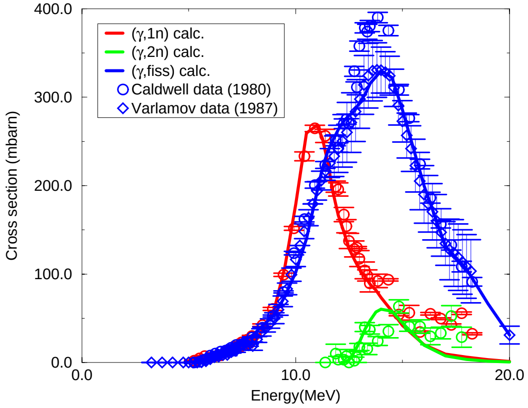

Fig. 7: Comparison between GNASH evaluations and experimental data for ^{235}U.

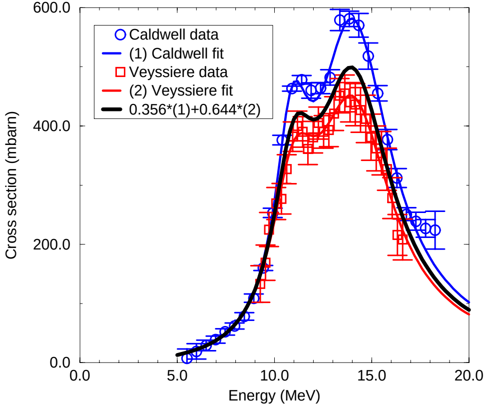

Fig. 8: Total photo-absorption cross section of 237Np.

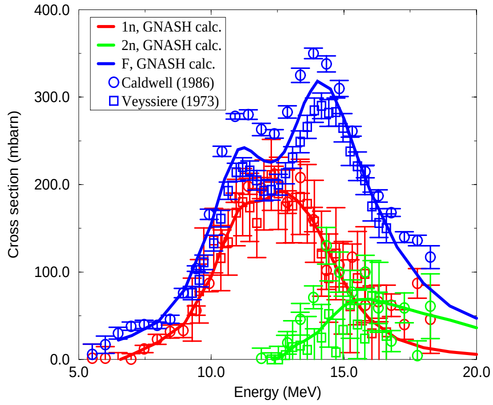

Fig. 9: Comparison between GNASH evaluations and experimental data for 237Np.

Our results for ^{237}Np partial channels obtained with GNASH are presented in Fig. 9. We have a rather good agreement with the experimental data for photoneutron production. For photofission, the evaluation remains between the two experimental data sets, what is coherent with our approach for photo-absorption. These new cross sections were included in the photonuclear activation data library for CINDER'90.

Predictions of photo-fission yields

Only few data exist on photo-fission fragment distributions. For ^{235}U and ^{238}U some mass and charge distributions are available. Only results for ^{235}U will be presented in this work.

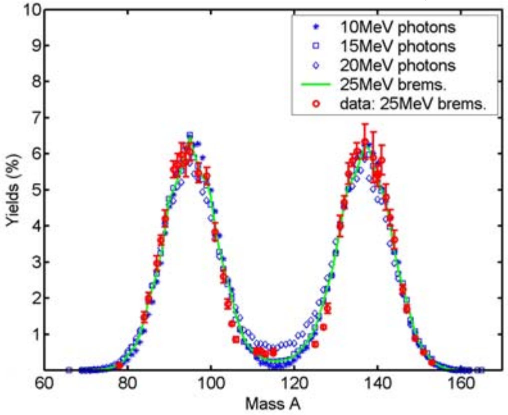

Fig. 10: Mass distributions for photofission of ^{235}U for different photon fluxes.

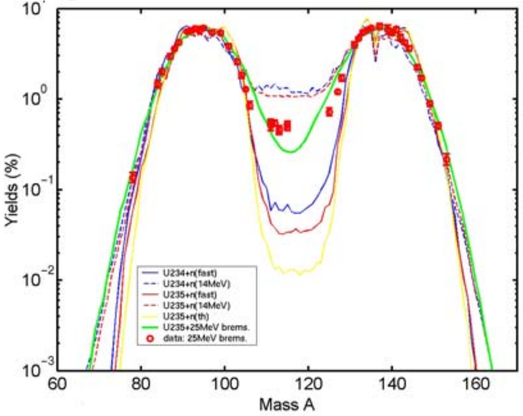

Fig. 11: Comparison of mass distributions for photo-fission of ^{235}U (green line) and neutron induced-fission for ^{234}U and ^{235}U.

Photo-fission fragment distributions are evaluated using the following procedure. The total photo-absorption cross section is calculated with the new evaluation as discussed above, after the GSI model is used to calculate competition between fission and evaporation. The nucleus de-excitation is performed with the ABLA code⁶⁾ to obtain the independent fission yields.

Our preliminary results for ^{235}U (see Fig. 10) are quite satisfactory: the data are reproduced both in peak positions, widths and absolute values. We also note that we found that the Bremsstrahlung photons from 25 MeV electrons (green lines) are equivalent to the 15 MeV mono-energetic photons (blue squares) as long as mass distribution of fission fragments is concerned.

It seems possible to find a systematic between neutron-induced fission and gamma-induced fission. We can deduce from Fig. 11 that for photo-fission of ^{235}U, fission of ^{234}U or ^{235}U by a 6-8 MeV neutron may be a good representation. However, similar comparison should be performed for other nuclei and for isotopic fission yield distributions in particular.

THE CASE STUDY: TRANSMUTATION OF NUCLEAR WASTE

To test CINDER'90 with the newly developed photonuclear activation data library we took as an example the transmutation analysis of nuclear waste. For each case study described below we simulate a sample in a photon flux environment of 10^{17} $\gamma.cm^{-2}.s^{-1}$ with a flat energy distribution between 10 and 20 MeV. The irradiation takes place for one year and is followed by 7 years of decay. The resulting activity is compared with the activity of the same sample after 8 years of decay, i.e. no irradiation at all. An advantage of using a photon flux instead of neutrons is that the mass of the element placed in the photon flux can only decrease, i.e. no higher elements than the mother nucleus are produced. The neutron flux due to photoneutron production in the sample was neglected in this study. For each case considered we also estimate an equivalent thermal and fast neutron fluxes giving similar decrease in remaining activity of the sample.

^{90}Sr ($T_{1/2}$=29 years) and ^{137}Cs ($T_{1/2}$=30 years)

^{90}Sr is one of the major contributors to the activity of nuclear waste during the first 100 years. Transmutation of ^{90}Sr and ^{137}Cs in photon fluxes has been studied by T. Matsumoto[8)]. We note separately that our results are in a good agreement with these calculations. This validates the library for the isotopes which belong to the transmutation chain of ^{90}Sr and ^{137}Cs.

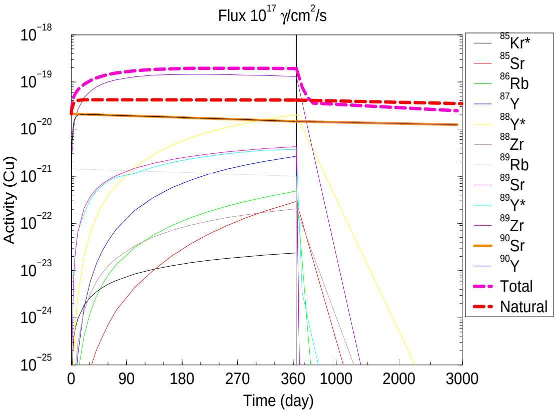

Fig. 12: Activity of the ^{90}Sr sample during 1 year irradiation and 7 years decay.

	Natural (ref)	After treatment	Equivalent neutron flux
Activity	1	0.7	$2x10^{16} n_{th}.cm^{-2}.s^{-1}$ $1x10^{17} n_{fast}.cm^{-2}.s^{-1}$

Table 1: Comparison of transmutation of ^{90}Sr in photon and neutron fluxes.

	Natural (ref)	After treatment	Equivalent neutron flux
Activity	1	0.33	$4x10^{17} n_{th}.cm^{-2}.s^{-1}$ $1.5x10^{18} n_{fast}.cm^{-2}.s^{-1}$

Table 2: Comparison of transmutation of ^{137}Cs in photon and neutron fluxes.

Fig. 11 presents activity of the main radioactive isotopes, created from ^{90}Sr, during one year of irradiation and 7 years of cooling. The observed activity decreases by 30% compared to the natural decay (no irradiation). The same results can be obtained with the thermal neutron flux of $2x10^{16} n_{th}.cm^{-2}.s^{-1}$ (also see Table 1). It is clear that the transmutation of ^{90}Sr is more efficient with neutrons. The neutron flux needed is 5 times lower than the photon flux.

After one year irradiation at 10^{17} $\gamma.cm^{-2}.s^{-1}$ and 7 years of cooling activity the sample is decreased by a factor of 3 compared to the natural decay. It seems that for ^{137}Cs transmutation by photons is more efficient than for ^{90}Sr. In addition, one would need a photon flux 4 times lower than a thermal neutron flux to obtain comparable transmutation efficiency (see Table 2).

Incineration of ^{237}Np

In this case, for transmutation of ^{237}Np, we do not compare the remaining activity as we did for fission products. Here we estimate the incineration rate by fission, i.e. number of actinides destructed by fission after 1 year of irradiation. Our results are summarised in Fig. 13. We found that to obtain the incineration rate of 5% per year the following photon and neutron fluxes are needed:

- $5\text{x}10^{16}\ \gamma.\text{cm}^{-2}.\text{s}^{-1}$
- $5\text{x}10^{14}\ \text{n}_{\text{th}}.\text{cm}^{-2}.\text{s}^{-1}$
- $2\text{x}10^{15}\ \text{n}_{\text{fast}}.\text{cm}^{-2}.\text{s}^{-1}$

Although all above flux intensities would be difficult to reach, one should not neglect the incineration by photons: we note that during the irradiation with photons no higher actinides will be created. This is not the case for the neutron based transmutation. Finally, we add that economical and technological criteria should be evaluated quantitatively, what is out of scope of this study.

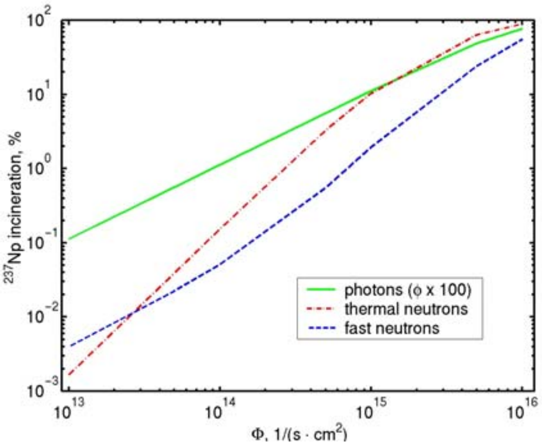

Fig 13: Incineration rate of ^{237}Np as a function of different photon and neutron flux intensities.

SUMMARY

The first version of the photonuclear activation data library for CINDER'90 has been constructed and is based on the IAEA evaluations, HMS-ALICE and GNASH calculations. The accuracy of the calculated and evaluated cross sections was assessed through comparisons with experimental data when available. The total photo-absorption cross section for actinides was improved. A number of preliminary activation calculations related to the transmutation of nuclear waste were performed to test the newly developed data library and its use by CINDER'90. A satisfactory agreement with published independent predictions was obtained.

The next step in the development of the photonuclear activation data library for CINDER'90 is to include photo-fission fragment distributions and corresponding delayed neutron yields. The GSI fission-evaporation code, also tested in part in this work, will be used for this purpose.

ACKNOWLEDGEMENTS

We gratefully acknowledge useful discussions with J. Benlliure and M. Blann. Part of this work was performed by M.L.G.M under the graduate student program during her stay at LANL.

References

[1] D. Ridikas, P. Bokov, M.-L. Giacri, "Potential Applications of Photonuclear Processes: Renewed Interest in Electron Driven Systems", Proc. of the Int. Conf. on Accelerator Applications/Accelerator Driven Transmutation Technology and Applications (AccApp/ADTTA'03), 1-5 June 2003, San Diego, California, USA.

[2] *Handbook on photonuclear data for applications, "*Cross section and spectra", IAEA-TECDOC-Draft No 3.

[3] M. Blann, "New pre-compound decay model", Phys. Rev. C*, **34** n°3, 1341 (1996).*

[4]W. B. Willson, **"**Recent development of CINDER'90 transmutation code and data library for actinides transmutation studies", GLOBAL'95 International Conference, Versailles, France, September 11-14

[5] P. G. Young et al., "*Comprehensive nuclear model calculation", Theory and use of GNASH* in "Nuclear reaction data and nuclear reactor – Physics, design and Safety – Vol 1", Int. Centre for Theoretical Physics, Trieste, Italy, April 15 - May 17 1999.

[6] A**.** R. Junghans et al.*,* **"**Projectile-fragment yields as a probe for the collective enhancement in the nuclear level density", Nucl. Phys. A ***629**, 635 (1998)*; J. Benlliure et al., "Calculated nuclide production yields in relativistic collisions of fissile nuclei", Nucl. Phys. *A **628**, 458 (1997).*

[7] S. S. Dietrich, B. L. Berman, *"Atlas of photoneutron cross sections obtained with monoenergetic photons",* Atomic data and nuclear tables ***38**, 199 (1988).*

[8] T. Matsumoto, "Calculations of gamma ray incineration of ^{90}Sr and ^{137}Cs", NIM A ***268**, 234 (1988).*